Journal of Applied Electrochemistry **31**: 1367–1372, 2001.

Electroless deposited Ni–Re–P, Ni–W–P and Ni–Re–W–P alloys

E. VALOVA[1], S. ARMYANOV[1], A. FRANQUET[2], A. HUBIN[2], O. STEENHAUT[2], J-L. DELPLANCKE[3] and J. VEREECKEN[2]

[1]*Institute of Physical Chemistry, Bulgarian Academy of Sciences, Sofia 1113, Bulgaria*
[2]*Vrije Universiteit Brussel, Dienst Metallurgie, Elektrochemie en Materialenkennis, B1050 Brussels, Belgium*
[3]*Université Libre de Bruxelles, Sciences des Matériaux et Electrochimie, B1050 Brussels, Belgium*

Received 2 May 2001; accepted in revised form 15 August 2001

Key words: electroless coatings, Ni–P based alloys

Abstract

Coatings of electroless Ni–W–P, Ni–Re–P and Ni–W–Re–P alloys were plated in alkaline citrate baths containing amino alcohols, but not free ammonia ions. The reference Ni–P alloy was used as an intermediate layer in the sandwich: Ni–Me–P/Ni–P/substrate. An extremely homogeneous thickness distribution of all alloy components was found by applying scanning Auger electron spectroscopy (SAES). The inclusion of refractory metals at the expense of nickel and without substantial change in phosphorus content was established. A non-oxidized state of the codeposited Re and W in Ni–W–P, Ni–Re–P and Ni–W–Re–P alloys was determined by means of X-ray photoelectron spectroscopy examination, as well as by SAES profiles, revealing the absence of oxygen throughout the coatings. All alloy films are amorphous and paramagnetic.

1. Introduction

It is well known that tungsten and rhenium have the highest melting points among metals. After the first attempts to introduce tungsten into electrolessly-deposited Ni–P alloys [1–3], attention was focused on their properties. It was observed that amorphous Ni–W–P alloys have good anticorrosive, protective behaviour [4–6] and high electrical resistance with low thermal resistance coefficient [7]. Electroless Ni–W–P alloy films have been used as heating components in low energy consumption thermal heads for printing devices [8]. Electrolessly deposited ternary alloys based on Ni–P and containing refractory metals W and Re as a third element have been reported to be suitable for microresistors [9].

Rhenium is nobler and deposits preferentially to nickel in the electroless plating of Ni–Re–P alloy [1]. It was observed that inclusion of rhenium up to 30 at % diminished the phosphorus content from 7 to 2 at % [10]. Amorphous Ni–Re–P alloys (up to 3.5 at % Re) were prepared using electroless deposition from acidic solution [11]. Increasing Re content has the same effect on the phosphorus concentration in coatings deposited from acidic solutions [11]. When tungsten rose from 0 to 20.8 wt % in Ni–W–P layers, phosphorus decreased from 14.0 to 6.2 wt % [12]. An X-ray photoelectron spectroscopy (XPS) study of electroless Ni–Re–P coatings showed that perrhenate ion from the solution was reduced to metallic Re inside the coating, where the presence of oxygen was negligible [13]. When the rhenium content was high enough, Ni–Re–P coatings exhibited non-magnetic properties and plasticity [10]. Ni–Re–P layers displayed a more noble electrochemical potential than Ni–P [10].

In view of the current and future applications of these alloys, several questions still need to be answered. The first question concerns whether the distribution of the refractory metals is uniform through the coating thickness. The second relates to the influence of Re and W on the content of phosphorus in the alloy and the third concerns the chemical status (oxidized or not) of the codeposited metals. The objectives of this work are to answer these questions and to attempt to achieve alloys with appreciable quantity of tungsten and rhenium, keeping the phosphorus content high.

2. Experimental details

The bath formulation was based on an alkaline citrate solution for electroless plating of Co–Ni–P alloy [14]. Sodium hypophosphite was applied as a reductor and nickel sulfate was used as Ni source (Table 1). The concentration of $NiSO_4 \cdot 6H_2O$ was doubled (0.106 M instead of 0.050 M) in bath A, used to plate Ni–P, in order to avoid Ni ion exhaustion, due to the higher deposition rate of the binary alloy. Sodium tungstate ($Na_2WO_4 \cdot 2H_2O$, 0.1 M) and potassium perrhenate (KRe_2O_7, 1.047×10^{-4} M) were added to the basic baths

Table 1. Basic bath compositions (M)

Bath	$NiSO_4 \cdot 6H_2O$	$NaH_2PO_2 \cdot H_2O$	Na-citrate
A	0.106	0.114	0.285
B	0.05	0.0855	0.095
C	0.05	0.114	0.285
D	0.05	0.114	0.19

B, C and D in order to plate ternary and quaternary alloys, respectively. Codeposition of refractory metals requires that the specific Me/Ni concentration ratio: W/Ni should be greater than unity, whereas Re/Ni should be very small, owing to the strongly preferential Re deposition. The following ratio of metal concentration (g L^{-1}) were chosen in our solutions for individual (of W or Re) and simultaneous (of both W and Re) codeposition: W/Ni = 6.3; Re/Ni = 6.6×10^{-3}. No stabilizers were used in the solutions for electroless plating of ternary and quaternary alloys.

Special attention was paid to the solution buffering and proper choice of complexing agents (citrate and amino-alcohols) to ensure pH stability in the alkaline region and to prevent precipitation of metal hydroxides [14]. The presence of free ammonia ion in the solution was avoided. This formulation had the advantage of allowing a direct comparison of coatings, containing refractory metals with the binary Ni–P alloy, deposited under identical conditions from a similar bath without addition of Re and W ions: bath A. This Ni–P film was applied as intermediate layer between the substrate and the Ni–Me–P coating and was referred as the 'EN underlayer'. All chemicals were pro analysis grade. Deionized water obtained from a Milli-Q system was used for solution preparation. The optimal plating parameters assessed by preliminary experiments were: bath temperature maintained constant at 89 ± 1 °C, and solution pH adjusted within 8.5–9.0 with H_2SO_4 or NaOH.

Several types of substrate, typically rectangular 20 mm × 10 mm coupons were used: (i) steel strips (specified as Fe), coupons of Al–Mg alloy AA5586 (denoted by Al), ceramic platelets coated by physical vapour deposition with thin Au film (designated as Au); and (ii) modified substrates comprising Al or Au substrates preplated with an EN underlayer and specified as Ni–P/Al, and Ni–P/Au, respectively. The very smooth Ni–P surface set the pattern for an extremely smooth appearance of the coatings plated on it.

Cleaning preceded the specific preplate treatment of all substrates. Steel substrates, after a standard electrocleaning, were immersed in 50% HCl solution for 60 s. Aluminium alloy substrates were subjected to a classic double zincate treatment and Au substrates were dipped for 30 s in a hot 50% H_2SO_4 solution. Each pretreatment step was followed by a thorough rinse with ordinary and deionized water. The modified substrates were submerged in the W or Re or W and Re-containing bath, immediately after the electroless deposition of Ni–P underlayer. The deposit thickness was assessed gravimetrically.

The chemical composition of the plated alloys was determined using energy dispersive X-ray spectroscopy (EDX) on a Jeol 733 and a Jeol JSM 820. Reflection high-energy electron diffraction (RHEED) technique was performed to examine the thin film structure. The B–H hysteresis loop tracer was employed for the determination of magnetic properties.

X-ray photoelectron spectroscopy (XPS or ESCA, electron spectroscopy for chemical analysis) was carried out in a PHI model 1600 system equipped with an Omni Focus Lens III using a standard Al K_α X-ray source (at a high voltage of 16 kV). The analysed area had a diameter of 0.4 mm and the take-off angle was 45 degrees. Sputter-etching by Ar^+ ions was applied at a beam voltage of 4.0 kV under a residual pressure of 15×10^{-3} Pa at 25 mA. The emission current was 20 mA and the sputtered area was 3 mm × 3 mm. The parameters of the multiplex survey were as follows: energy pass 29.35 eV; step size 0.10 eV; time/step 50 ms; repeats 35.

Scanning Auger electron spectroscopy (SAES) was performed using a PHI model 650 scanning Auger electron microscope with a cylindrical mirror analyser (CMA) for Auger electron detection. PHI PC-Access 7.0 software was applied to collect the spectra yielding quantitative profiles. The subsequent data treatment was performed with PHI Multipak 5.0 A software. The following working conditions for SAES were used: primary accelerating voltage: 3 kV; source: LaB_6 cathode; beam current: 100 nA (spot size about 0.5 μm); magnification: ×1000; CMA energy resolution: 0.6%; high vacuum in the chamber: 6.7×10^{-9} Pa. Ion sputtering conditions were: accelerating voltage 3.5 kV; ion beam current 25 mA; Ar gas pressure 2×10^{-4} Pa; vacuum during sputtering with Ar gas: 6.7×10^{-7} Pa; raster surface: 1 mm × 1 mm; tilt angle sample: 30°.

3. Results and discussion

The elemental composition of the alloys can be seen in Tables 2 and 3, where selected data for two types of substrate are presented. It is clear from Table 2, that decrease in citrate concentration (from solution C to D and B, see Table 1) reduces the phosphorus content and increases the deposition rate. To obtain high phospho-

Table 2. Chemical composition (by EDX) of electroless deposited Ni–W–P and Ni–P coatings deposited on a steel substrate

Sample	Bath	pH	Thickness /μm	Rate /μm h^{-1}	Ni /wt %	P /wt %	W /wt %
NiP	A	8.5	13.0	13	89.8	10.2	–
NiWP3	C	8.5	0.85	1.4	75.9	10.6	13.5
NiWP2	D	8.5	1.6	1.6	76.3	6.8	16.9
NiWP1	B	9.0	2.7	5.2	84.8	4.5	10.7

Table 3. Chemical composition (by EDX) of electroless deposited Ni–P as well as Ni–W–P, Ni–Re–P, and Ni–W–Re–P coatings deposited on Al preplated with electroless Ni–P

Sample	Bath	pH	Rate /μm h^{-1}	Thickness /μm	Ni /wt %	P /wt %	W /wt %	Re /wt %
NiP	A	8.5	11	11	90.9	9.1	–	–
NiWP	C	8.5	0.7	0.9	77.8	9.9	12.2	–
NiReP	C	8.5	0.3	0.5	77.8	13.0	–	9.2
NiWReP2	C	8.5	0.5	0.7	80.7	12.2	4.0	3.1
NiWReP3	C	8.5	0.5	2.1	80.9	13.3	2.6	3.2

rus coatings most of the experiments were performed with bath C, that is, with the highest citrate concentration. All Ni–Me–P coatings in sandwich systems with Ni–P intermediate film shown in Table 3 were plated in bath C. The introduction of W, Re or W + Re in coatings deposited from solution C does not noticeably change the percentage of phosphorus, as can be seen in Tables 2 and 3. Usually the third component in electroless Ni–Me–P coatings reduces the phosphorus content, and this effect is pronounced especially in Ni–Zn–P alloys [15, 16].

Although Tables 2 and 3 illustrate the mentioned trends, we need to point out that EDX should be applied cautiously for the determination of the elemental composition in this particular case. The reason for this is illustrated in Figure 1, showing typical EDX spectra of Ni–P and Ni–P-based alloy samples. The main characteristic peaks are too close and/or overlapping. At the same time the Re and W peaks are rather weak due to the small metal quantity. The low deposition rate, especially in the case of Re-incorporating alloys made it too time consuming to obtain massive samples. This renders the EDX results presented in the Tables 2 and 3 semiquantitative.

Magnetic properties examination was performed with coatings of Ni–W–P, Ni–Re–P and Ni–Re–W–P with an intermediate Ni–P high phosphorus layer deposited on paramagnetic Al substrate. All samples exhibited paramagnetic behaviour (i.e., no hysteresis loop was displayed). This is related to an amorphous structure, similar to that of the intermediate high phosphorus Ni–P films [15]. A RHEED study revealed the amorphous structure of the alloy films, since only halos were obtained. Thus the magnetic behaviour and the structure characterization of the alloys under consideration proved to be consistent, as was found in many investigations of Ni–P and Ni–P-based electroless deposits (e.g., see [15]). Amorphous structure was also observed by XRD of electrolessly deposited Ni–W–P alloy films of W content close to that reported in this work, but embodying substantially less phosphorus [17].

As illustrated in Figure 2, an extremely homogeneous distribution of alloy components was observed. It was established that the incorporation of tungsten occurred at the expense of nickel and with a very small decrease in the phosphorus content, as seen from the descending profiles of nickel and phosphorus at the interface Ni–P/Ni–W–P: Figure 3. A significant quantity of oxygen was only observed at the sample surface: (Figures 2 and 3).

A uniform tungsten distribution through film thickness was also displayed in Auger depth profiles of Ni–W–P films electrolessly deposited onto GaAs [18]. The authors also detected a distinct difference in the composition of thin (about 0.8 μm) and thick (about 8 μm) films.

The addition of rhenium did not change the homogenous distribution of alloy components. Its inclusion

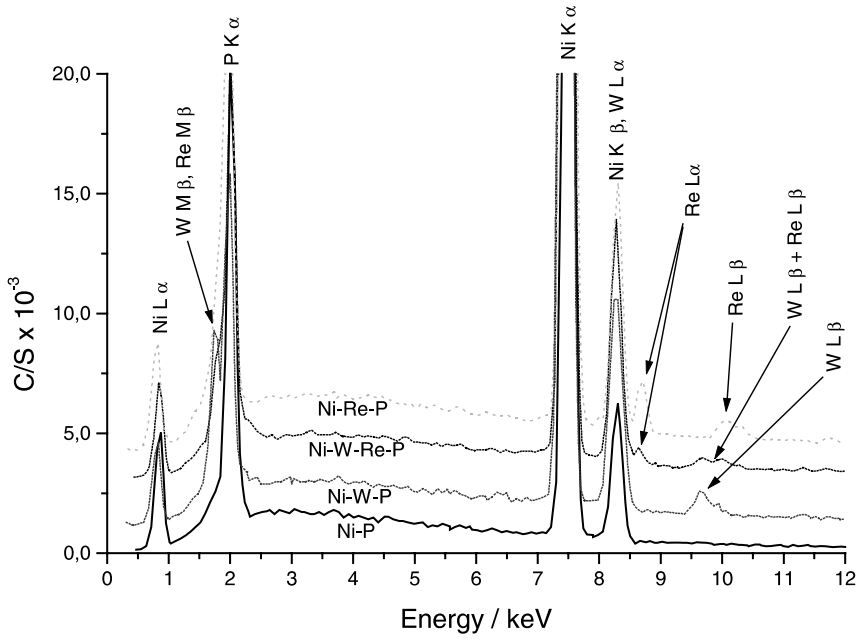

Fig. 1. EDX spectra of Ni–P, Ni–W–P, Ni–Re–P and Ni–W–Re–P films. Spectra are superimposed to illustrate overlapping or proximity of all relevant characteristic peaks, causing limited applicability of the method for quantitative chemical analysis in this case.

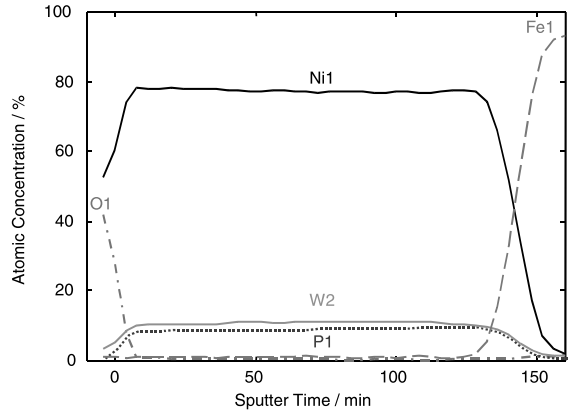

Fig. 2. Auger sputter-etch depth profiles of Ni, W, O and P components of a Ni–W–P coating deposited onto an iron substrate.

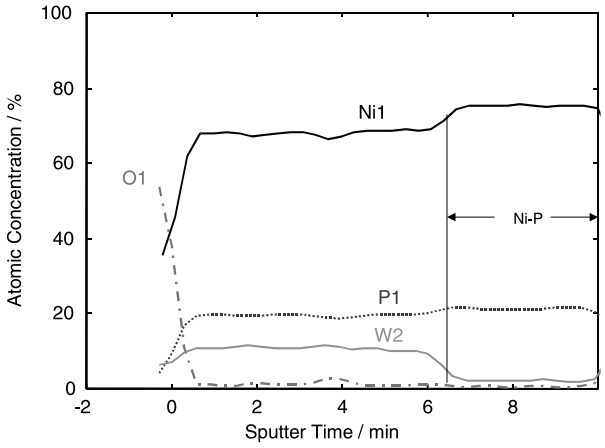

Fig. 3. Auger sputter-etch depth profiles of Ni, W, O and P components of a Ni–W–P coating deposited onto Ni–P substrate.

was again at the expense of nickel. However, in contrast to the case with W, there was no reduction in phosphorus content (Figure 4). When both tungsten and rhenium were included with a larger concentration of Re in the alloy, there was no reduction in phosphorus content: (Figure 5).

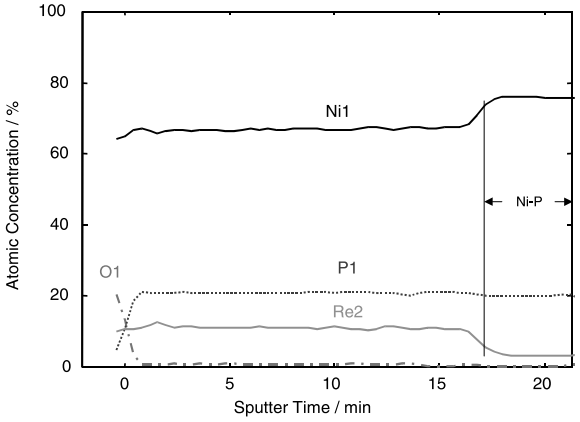

Fig. 4. Auger sputter-etch depth profiles of Ni, Re, O and P components of a Ni–Re–P coating deposited onto Ni–P substrate.

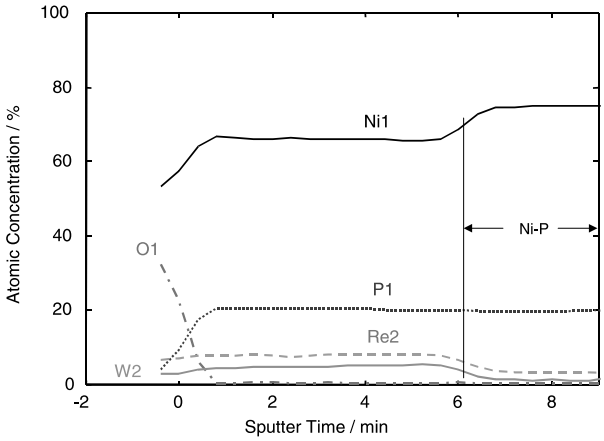

Fig. 5. Auger sputter-etch depth profiles of Ni, W, Re, O and P components of a Ni–Re–W–P coating deposited onto Ni–P substrate.

The absence of oxygen throughout the coatings, as shown by SAES profiles (see Figures 2–5) did not provide evidence for some oxidized species of the codeposited Re and W. The presence of oxygen, as well as of carbon, in the Auger depth profiles of electroless Ni–W–P coatings in substantial quantity on the surface, which is gradually diminishing while approaching the substrate, was explained by the greater absorption activity of a freshly deposited film [19].

To examine the chemical condition of alloy components the ESCA data from the software of PHI Multipak 5.0 A were selected as reference. According to usual practice, in each XPS experiment the position of C_{1s} was taken as a starting point to determine the experimental (systematic) peak shift in respect to the reference binding energy (BE) values. The correction factor was found by subtracting the reference value from the experimental value for C_{1s}. This factor (indicated in Table 4 for each sample at the levels C_{1s}) was then subtracted from the measured BE values for W, Re, P, and Ni and the results are presented as 'Experimental after shift correction'. In the last column the experimental and the reference differences between the binding energies (i.e., the spin doublet separation) of levels $Ni_{2p1/2}$ and $Ni_{2p3/2}$, $W_{4f5/2}$ and $W_{4f7/2}$ and $Re_{4f5/2}$ and $Re_{4f7/2}$, respectively, are given.

The data presented in Table 4 show that W and Re are predominantly in the non-oxidized state in the investigated alloys, since no significant deviation of experimental from reference values is observed, either in the binding energy or in the spin doublet separation. If a state of high oxidation prevailed a shift would be observed in the binding energy that might reach several electronvolt for lines $W_{4f7/2}$ and $Re_{4f7/2}$ in the oxides [20].

The peak form (Figures 6–8) does not show an oxidation state being very close to the reference for the metallic state. The results of XPS examination are in agreement with the observations made by means of scanning Auger electron spectroscopy and depth profiling. They are in accordance with data for Re in

Table 4. Data for binding energy: experimentally measured and corrected on the base of reference values from PHI Multipak 5.0 A software (*11.spe files)

Sample	Peak	Binding energy, *BE*/eV			W or Re $BE_{4f5/2}$–$BE_{4f7/2}$; Ni $BE_{2p1/2}$–$BE_{2p3/2}$ Doublet separation/eV
		Experimental	Reference	Experimental after the shift correction	
NiWReP2 before sputtering	C_{1s}	288.7	284.3	284.3 = 288.7–4.4	
	$W_{4f7/2}$	35.4	31.2	31.0	Experimental 2.4
	$W_{4f5/2}$	37.8	33.4	33.4	Reference 2.2
	$Re_{4f7/2}$	44.7	40.3	40.3	Experimental 2.4
	$Re_{4f5/2}$	47.1	42.7	42.7	Reference 2.4
NiWReP2 after 15 min of sputtering	$W_{4f7/2}$	35.5	31.2	31.1	Experimental 2.2
	$W_{4f5/2}$	37.7	33.4	33.3	Reference 2.2
	$Re_{4f7/2}$	44.5	40.3	40.1	Experimental 2.4
	$Re_{4f5/2}$	46.9	42.7	42.5	Reference 2.4
NiReP2 before sputtering	C_{1s}	289.7	284.3	284.3 = 289.7–5.4	
	$Re_{4f7/2}$	45.2	40.3	39.8	Experimental 2.5
	$Re_{4f5/2}$	47.7	42.7	42.3	Reference 2.4
NiReP2 after 50 min of sputtering	$Re_{4f7/2}$	45.1	40.3	39.7	Experimental 2.5
	$Re_{4f5/2}$	47.6	42.7	42.2	Reference 2.4
NiWP2 after 30 s of sputtering	C_{1s}	285.1	284.3	284.3 = 285.1–0.8	
	$W_{4f7/2}$	31.5	31.2	30.7	Experimental 2.2
	$W_{4f5/2}$	33.7	33.4	32.9	Reference 2.2
NiWP2 after 20 min of sputtering	$W_{4f7/2}$	31.3	31.2	30.5	Experimental 2.3
	$W_{4f5/2}$	33.6	33.4	32.8	Reference 2.2
NiWP4 after 30 min of sputtering	C_{1s}	288.2	284.3	284.3 = 288.2–3.9	
	$W_{4f7/2}$	34.7	31.2	30.8	Experimental 2.2
	$W_{4f5/2}$	36.9	33.4	33.0	Reference 2.2
	P_{2p}	132.9	129.3	129.0	
	$Ni_{2p3/2}$	855.7	852.7	851.8	Experimental 17.3
	$Ni_{2p1/2}$	873.0	869.9	869.1	Reference 17.2

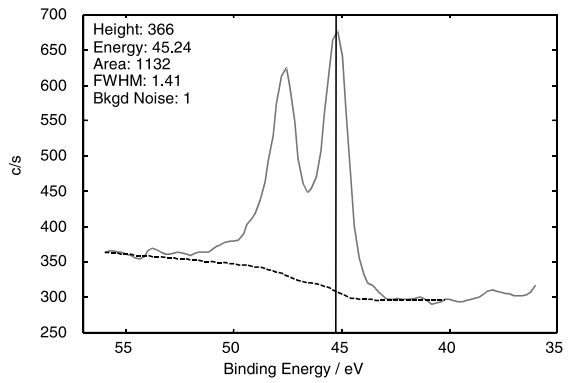

Fig. 6. XPS $Re_{4f5/2}$ and $Re_{4f7/2}$ spectrum from surface of sample NiReP2 before sputtering. Details in Table 4.

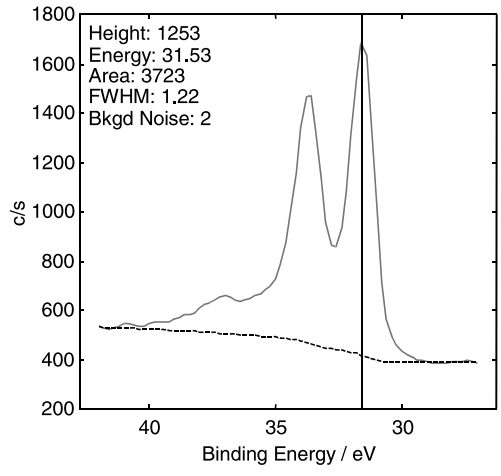

Fig. 7. XPS $W_{4f5/2}$ and $W_{4f7/2}$ spectrum from sample NiWP2 after 30 s of sputtering. Details in Table 4.

electroless Ni–Re–P [13], where the partially oxidized state of Re has only been observed on the surface. It should be emphasised that, in electrodeposited Ni–W, tungsten may be present in oxide form, this being the predominant form in some cases [21]. However, in electrodeposited amorphous Ni–W–P films of higher tungsten content (20–40 wt %) it is apparently in metallic form [22]. Nevertheless, it was shown recently by XPS, that in $Ni_{80.4}W_{1.5}P_{18.1}$ powders produced by chemical reduction (electrolessly), the included tungsten could appear in both metallic and oxidized state (as tungstate) [23].

This diversity in the states of tungsten emphasizes the importance of studying the valence condition of the codeposited refractory metals, which could affect the catalytic as well as corrosion behavior of the nickel-based alloys [23].

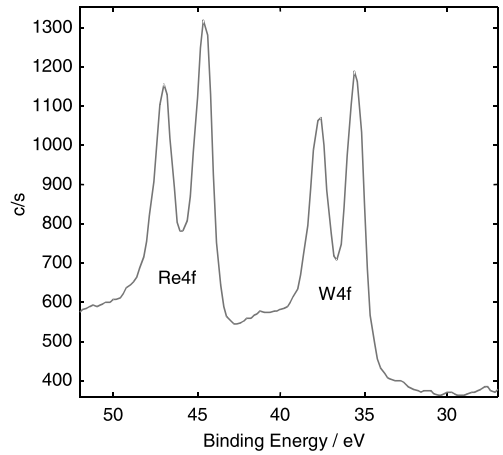

Fig. 8. XPS $Re_{4f5/2}$, $Re_{4f7/2}$, $W_{4f7/2}$ and $W_{4f7/2}$ spectrum from sample NiWReP2 after 15 min of sputtering. Details in Table 4.

4. Conclusions

Ni–P based ternary and quaternary alloys of high phosphorus content, containing the refractory metals W, Re and both together, were electrolessly deposited in alkaline citrate solutions using various materials as substrate. Studies of these types of alloy by means of SAES revealed an extremely uniform compositional thickness distribution. SAES profiles of the alloys deposited on homogeneous, amorphous, highly polished electroless Ni–P films demonstrated that W and Re inclusion proceeded at the expense of Ni, providing a prerequisite for obtaining coatings of high phosphorus embodiment. The combined SAES–XPS examination proved incorporation of both refractory metals predominantly in metallic form. These types of alloy are paramagnetic and amorphous. Their characteristics are favourable for possible application as materials of high electrical resistance with low temperature coefficient and good corrosion resistivity.

Tungsten slightly decreased the phosphorus content and lowered the electroless deposition rate in comparison with the binary Ni–P alloy. Rhenium showed a complex behaviour in used citrate bath: its deposition was highly preferential to Ni, but proceeded at significantly reduced total plating rate. Under the applied conditions Re appeared not to impede phosphorus codeposition. Rhenium electrochemistry is far from being well studied and its role in the most complicated electroless deposition process needs more detailed investigation. However, the present study demonstrates the different action of W and Re codeposition in electroless Ni–P based alloys, as compared with Zn [15, 16].

Acknowledgements

This research was made within the frames of a joint project supported by the Commissariat Général aux Relations Internationales de la Communauté Française de Belgique and Bulgarian Academy of Sciences.

References

1. F. Pearlstein and R.F. Weightman, *Electrochem. Technol.* **6** (1968) 427.
2. G.O. Mallory, *Trans. Inst. Metal Finish.* **52** (1974) 156.
3. G.O. Mallory and T.R. Horhn, *Plat. Surf. Finish.* **66**(4) (1979) 40.
4. K. Aoki and O. Takano, *J. Metal Fin. Soc. Jap.* **35** (1984) 460.
5. K. Aoki and O. Takano, *Plat. Surf. Finish.* **73**(5) (1986) 138.
6. Z. Bangwai, H. Wangyu, Q. Xuanyuan, Z. Qinglong, Z. Heng and T. Zhaosheng, *Trans. Inst. Metal Finish.* **74**(2) (1996) 69.
7. K. Aoki and O. Takano, *Plat. Surf. Finish.* **87**(3) (1990) 48.
8. H. Sawai, T. Kanamori, I. Koiwa, S. Shibata, K. Nihei and T. Osaka, *J. Electrochem. Soc.* **137** (1990) 3653.
9. T. Osaka and J. Kawaguchi, *in* N. Masuko, T. Osaka and Y. Ito (Eds), 'Electrochemical Technology: Innovation and New Developments' (Kodansha and Gordon and Breach, Tokyo, 1996), pp 3–16.
10. I. Genutiene, A. Luneckas and J. Lenkaitiene, *Zashchita Metallov* (in Russian) **22** (1986) 748.
11. D. Mencer, *J. Alloys Compd.* **306**(1–2) (2000) 158.
12. I. Koiwa, M. Usuda and T. Osaka, *J. Electrochem. Soc.* **135** (1988) 1222.
13. I. Genutiene, J. Lenkaitiene, Z. Jusis and A. Luneckas, *J. Appl. Electrochem.* **26** (1996) 118.
14. S. Armyanov, G. Chakarova, T. Vangelova and Ts. Pojarlieva, *Bulgarian Patent 47 282* (1986).
15. E. Valova, I. Georgiev, S. Armyanov, J-L. Delplancke, D. Tachev, Ts. Tsacheva and J. Dille, *J. Electrochem. Soc.* **148** (2001) C266.
16. E. Valova, S. Armyanov, A. Franquet, O. Steenhaut, A. Hubin, J-L. Delplancke and J. Vereecken, *J. Electrochem. Soc.* **148** (2001) C274.
17. L.I. Stepanova, T.I. Bodrykh and V.V. Sviridov, *Metal Finish.* **99**(1) (2001) 50.
18. L.I. Stepanova, L.V. Barkovskaya and O.G. Purovskaya, *Metal Finish.* **93**(1) (1995) 26.
19. L.I. Stepanova, T.I. Bodrykh, V.V. Sviridov and L.S. Ivashkevich, *Zh. Prikl. Khimii* (*Russian J. Appl Chem.*) **69**(12) (1996) 1951.
20. C.D. Wagner, *in* D. Briggs and M.P. Seah (Eds), 'Practical Surface Analysis', Vol. 1, (J. Wiley & Sons, New York, 2nd edn, 1990).
21. G. Rauscher, V. Rogoll, M.E. Baumgaertner and Ch. J. Raub, *Trans. Inst. Metal Finish.* **71**(3) (1993) 95.
22. S. Yao, H. Guo and M. Kowaka, *Electrochem. Soc. Ext. Abstr.* **93-1** (1993) 235.
23. Song, X. Bao and M. Muhler, *Appl. Surf. Sci.* **148** (1999) 241.